MODELING OF TWO DIFFERENT TYPES OF WIND TURBINES

Dr. Rafid M. Hannun
Lecturer/ Mechanical Eng. Dept., College of Engineering, Thi-Qar University
Email: eng_rafid005@yahoo.com

ABSTRACT
There are many kinds of wind mills and turbines. In this study, practical rig models of two turbines were manufactured at Nassiriya city (31.036^o N, 46.21^o E) to compare their work with other related properties and fundamentals. The first is vertical axis wind turbine called Savonius rotor (S- rotor) with dimensions (1500*500*8) mm, the second is horizontal axis wind turbine has a components of plastic blade, steel bearing, steel base, steel shaft, bearings and pointed blade, the plastic blades erected on steel support of length 210 mm. Theoretical analysis of turbines motion were presented in wide manner of explanation. The readings of the two turbines were done in 2nd, 3rd, 8th March and 2nd, 4th April , 2011for many parameters of motion, angular velocity, linear velocity, kinetic energy, air mass flow rate and mechanical power. The results of wind velocity were compared with metriological data in Nassiriya city. The maximum amount of power was 4.65 Watt calculated for horizontal axis turbine. FLUENT and GAMBIT codes were used to prove the validity of this study. It was concluded that the horizontal axis turbine is more efficient than the vertical one, which is in good agreement with literature.

KEYWORDS: Wind, Turbine, Mills, Wind Energy, Wind Power, Savonius-Rotor

نـمـذجـة عنـفـتين ريحـيتين مختلـفـتين

الباحث م.د. رافد معلك حنون/ كلية الهندسة– جامعة ذي قار–قسم الهندسة الميكانيكية

الموجز

توجد عدة انواع من طواحين الهواء والزعنفات الريحية. في هذه الدراسة، تم تصنيع نموذجين عمليين من الزعنفات الريحية في مدينة الناصرية (31.036 درجة شمال خط الاستواء، 46.21 درجة شرق خط كرنيش) وذلك لأجراء مقارنة عملية لعملهما والخواص والاساسيات الاخرى فيهما. كان النموذج الاول لعنفة ريحية عمودية المحور والتي تسمى بدوامة سافونيوس بأبعاد (8*500*1500) ملم ، أما الثانية فكانت من نوع الزعنفة الريحية افقية المحور والتي تتكون من زعنفة بلاستيكية ومحمل حديدي وقاعدة حديدية ومحور حديدي ومثبتات للمحامل وزعانف بلاستيكية ثبتت على محور حديدي بطول 210 ملم. تم تقديم تحليل رياضي نظري لحركة الزعنفة بشكل واضح وواسع. اخذت القراءات لعدة ايام تم ابراز بعضها في هذا البحث للأيام 2، 3، 8 آذار و 2، 4 نيسان من عام 2011 ولعدة خواص من خواص الحركة كالسرعة الزاوية والسرعة الخطية والطاقة الحركية ومعدل الجريان الكتلي للهواء والقدرة الميكانيكية. تمت مقارنة النتائج التي تم الحصول عليها لسرعة الرياح مع بيانات الرصد الجوي

والانواء الجوية في مدينة الناصرية. اقصى قدرة تم الحصول عليها هي 4.65واط للزعنفة الافقية. استخدم برنامج FLUENT و GAMBIT لبرهنة وجودية الدراسة مع المقاييس العلمية. كذلك تم استنتاج ان الزعنفة الافقية هي اكفأ من العمودية وذلك كان متوافقاً مع أدبيات الموضوع السابقة.

NOMENCLATURE

Symbol	Definition
A	Cross sectional area of air cylinder (m^2)
C_p	The dimensionless power coefficient
Eq.	Equation
Fig.	Figure
KE	Kinetic energy of wind mill (m^2/s^2)
ΔKE	The change in kinetic energy of wind mill (m^2/s^2)
ΔL	The length of air cylinder (m)
V	The speed of the wind (m/sec)
Δt	Time interval (sec)
P	Wind power (Watt)
R	Radius of the rotor (m)
m	Mass of the air (kg)
Δm_{air}	The change of air mass (kg)
β	The ratio of down wind velocity to up wind velocity (dimensionless)
ρ	The destiny of air (kg/m^3)

INTRODUCTION

Wind energy is a potential source of energy. Wind is the motion caused by uneven heating of the earth's surface by the sun and rotation of the earth. It is generated due to various global phenomena such as, air –temperature difference, associated with different rates of solar heating. Since the earth's surface is made up of land, desert, water and forest areas. The surface absorbs the suns radiation differently. Locally, the strong winds are created by sharp temperature difference between the land and the sea (**Smith, 1989**). Modern wind turbines are classified as either horizontal axis or vertical axis. A vertical axis turbine has blades that rotate around a vertical axis, and its visual appearance has been likened to an eggbeater. A horizontal axis turbine has blades that rotate around a horizontal axis. Horizontal axis turbines are the most common turbines in use (**Johnson, 2006**).

(**Percival et. al., 2009**) presented an exploration of a Savonius rotor (S-rotor) wind turbine adapted for household/domestic electricity generation. The design process and justification of the new machine was described. A prototype has been built and installed at a selected site. The operational experience of this site testing was also summarized.

The power of darrieus type wind turbine considering real air velocity on the wind turbine blade was predicted by (**Du Lian et. al., 2010**) that found the local blade Reynolds number application increasing the accuracy in the region of higher tip speed ratio that can be applied widely in the wind power industry.

(**Sheldahl, 1981**) presented a 2-m-dia Darrieus Vertical Axis Wind Turbine which was extensively tested in the Vought Corporation Low Speed Wind Tunnel. It was operated to determine if field data corresponds to data obtained in the wind tunnel. It is believed that the accuracy of the wind tunnel test data was verified and thus the credibility of that data base was further established.

(**Schultz, 2009**) applied a common set of requirements to a variety of potential gearbox designs for a 2.0mWwind turbine and compared the resulting "geared component" weights, gearbox envelope sizes, generator sizes, and generator weights.
(**Stiesdal, 1999**) showed many components of wind turbines, the aerodynamics of the wind turbine, the transmission system, the generator and control and safety systems.
(**DeCoste et.al., 2007**) designed, fabricated and tested a Darrieus wind turbine which starts solely from the energy of the wind at Dalhousie University.

RIG FABRICATION OF WIND TURBINES

Manufacturing of Vertical Axis Wind Turbine

The major components are Aluminum blades, steel support, rotor shaft, four ball bearings and four long bolts. The plate of wind fan is shaped as (S) character to create Savonius rotor (S-rotor) wind turbine with dimensions (1500*500*8) mm. This fan is erected at the end of a steel shaft without welding. The steel shaft is fastened on a steel structure by using the ball bearing for top and bottom parts.

Manufacturing of Horizontal Axis Wind Turbine

The major components are plastic blades, steel bearings, steel base, steel shaft, bearings and pointed blade. The plastic blades are erected on a steel support of length 210 mm in vertical support by bearings for facilitating motion of blades. So, it is supported on a horizontal steel structure with a shaft of length 325mm at the end. There is the steel edge (120, 150, 10) mm with length 103m m for steering the wind turbine in the direction of wind. All parts are fastened on the steel base and structure.

THEORETICAL ANALYSIS

A typical horizontal axis turbine consists of a rotor with two or more blades attached to machine cabin set on top of a post that is mounted on a foundation block. The machine cabin contains a generator attached to the wind turbine. The rotor blades can rotate in the vertical plane and the machine cabin can rotate in the horizontal plane. The ability of the turbine –generator assembly to rotate around a vertical axis is called the yaw effect. The angle between the rotor blades and the plane of rotation of the rotor blades is the pitch angle. The pitch angle of the rotor blades can be used to control the rotation rate of the rotor blade **[(Wilson, 1994), (Nasuk et. al., 1983), (Hanson et. al., 1993) and (Masse, 1986)]**.
Figure 5 illustrates a cylinder of air approaching a rotating horizontal axis wind turbine. The cylinder of air shown in **Figure** 5 has the volume

$$\Delta V = A\Delta L \tag{1}$$

Where A is the cross –sectional area and ΔL is the length of cylinder of air. If the density of air ρ_{air} is approximately constant, the mass of cylinder of air is

$$\Delta m_{air} = \rho_{air}\Delta V = \rho_{air} A\Delta L \tag{2}$$

Suppose the cylinder of air in **Figure** 5 is moving with speed v_{air} directly at the turbine. The air speed v_{air} is the speed of wind. The kinetic energy of the moving air is

$$\Delta KE_{air} = \frac{1}{2}\Delta m_{air} v_{air}^2 = \frac{1}{2}\rho_{air} A\Delta L v_{air}^2 \tag{3}$$

The length ΔL of the cylinder of air that reaches the wind turbine in a time interval Δt is

$$\Delta L = v_{air} \Delta t \tag{4}$$

Substituting Equation (4) into Equation (3) gives

$$\Delta KE_{air} = \frac{1}{2} \rho_{air} A v_{air}^3 \Delta t \tag{5}$$

The rate of arrival of air is the wind power, or

$$P_{wind} = \frac{\Delta KE_{air}}{\Delta t} = \frac{1}{2} \rho_{air} A v_{air}^3 \tag{6}$$

Wind power is proportional to the cube of wind speed.
The area A is the surface area of the circle formed by the rotating tip of the rotor blade. If the rotor blade has radius R, the area is

$$A = \pi R^2 \tag{7}$$

Substituting Equation (7) into Equation (6), the wind power:

$$P_{wind} = \frac{\pi}{2} \rho_{air} R^2 v_{air}^3 \tag{8}$$

Equation (8) shows that wind power is proportional to the square of the radius of the fan created by the rotating rotor blade.
In this analysis, it is assumed that the wind direction is orthogonal to the plane of rotation of the rotor blade. Thin rotor blade is assumed. The gyroscopic couple may affect the wind turbine as a result of change in wind direction. The wind speed is seldom constant; it can vary from still to tornado or hurricane speed. The speed of rotation of the tip of the wind turbine is

$$v_{tip} = Rw \tag{9}$$

Where w is the angular velocity of the turbine.

Electrical power output from a wind turbine is a product of the efficiency η_{wind} times the input wind power. The optimum power output is approximately [2]:

$$P_{out} = \eta_{wind} P_{wind} = \frac{\pi}{2} \eta_{wind} \rho_{air} R^2 v_{air}^3 \tag{10}$$

The efficiency η_{wind} depends on several factors: the efficiency of converting mechanical energy of the rotor blade into electrical energy, the reliability of the wind turbine and the rate of rotation of the rotor blade.

It is assumed that the kinetic energy of the wind incident on the turbine is converted to rotational energy of the rotor blades. The kinetic energy of the moving air that is extracted for power production is

$$\Delta KE_{air} = \frac{1}{2}\Delta m_{air}(v_{upwind}^2 - v_{downwind}^2) \tag{11}$$

The mass of air that is needed to move the rotor blade in a time interval Δt is

$$\Delta m_{air} = \rho_{air} A v_{actuate} \Delta t \tag{12}$$

Where $v_{actuate}$ is the wind velocity that actuates the rotor and A is the cross sectional area shown in **Figure** 1 and **Figure** 5. Therefore:

$$v_{actuate} = \frac{v_{upwind} + v_{downwind}}{2} \tag{13}$$

Substituting Equations (12) and (13) into equation (11) gives

$$\Delta KE_{air} = \rho_{air} A \frac{v_{upwind} + v_{downwind}}{2}(v_{upwind}^2 - v_{downwind}^2)\Delta t \tag{14}$$

The extracted wind power is

$$P_{extracted} = \frac{\Delta KE_{air}}{\Delta t} = \frac{1}{2}\rho_{air} A \frac{v_{upwind} + v_{downwind}}{2}(v_{upwind}^2 - v_{downwind}^2) \tag{15}$$

Equation (15) can be written in the simplified form

$$P_{extracted} = \frac{1}{4}\rho_{air} A v_{upwind}^3 [1 + \beta_{wind} - \beta_{wind}^2 - \beta_{wind}^3]$$
$$= C_P \cdot \frac{1}{2}\rho_{air} A v_{upwind}^3 \tag{16}$$

Where $\beta_{wind} = v_{downwind} / v_{upwind}$ is the ratio of downwind velocity to upwind velocity, and C_P is the dimensionless power coefficient

$$C_P = \frac{1}{2}[1 + \beta_{wind} - \beta_{wind}^2 - \beta_{wind}^3] \tag{17}$$

The power coefficient is typically in the range $0 \le C_P \le 0.4$ for actual wind turbines.
A theoretical maximum power coefficient is obtained by:

$$\frac{dP_{extracted}}{d\beta_{wind}} = 0 \tag{18}$$

For β_{wind}. the physically meaningful solution to eq. (18) is

$$(\beta_{wind})_{\max} = \frac{1}{3} \tag{19}$$

Substituting Equation (19) into Equation (17) gives the power coefficient

$$(C_P)_{\max} = \frac{16}{27} \approx 0.593 \tag{20}$$

Equation (20) is the theoretical maximum power coefficient and is called Betz' limit. It is approximately 59.3% of the power in the wind which is the maximum percentage of the wind power that can be extracted (**FLUENT, 2008**). In this paper, the values of C_P are found by equation (17) to be limited between 0.59 to 0.13 for different readings of turbines.
In addition to the horizontal axis wind turbine analysis previously mentioned, the vertical axis differs in projected area where the wind affects it. Herein, the area is 50×50 cm and the other parameters are the same. This movement of turbine has starting velocity for continuous movement with any direction.

RESULTS AND DISCUSSION:
The findings of this paper were accomplished in Nassiriya city region (31.036^o N, 46.21^o E). This city has high ranges of wind speed along the year. The readings were recorded at different hours and days with same location by using a laser anemometer. The metrological data of wind speed were taken to compare the results of this study from metrology center in Nassiriya.
Figure 6 shows the angular velocity readings for the two turbines in 8th March 2011, the vertical turbine has high values for all readings because its diameter is larger than the other, so, its actuated area is larger to increase the rotating torque resulted due to wind force by affected area.
The angular velocity readings of turbines for five days of measurements are shown in **Figure** 7. Also, as in **Figure** 6 the vertical turbine rig has higher angular velocity values than that for horizontal axis turbine due to the difference in affected area for both turbines. The general curves line equations give that (y=0.166x+34.228) line equation of vertical axis turbine and (y=0.1433x+22.179) for the horizontal axis turbine which was found by using MS. Excel Operating System Programmer. This gives 34.228 rpm as minimum value of the vertical and 22.179 rpm for horizontal one.
It is observed that the curves have similar general inclination for all findings of the two turbines which give good validity of readings. The actuated area of the vertical and horizontal axis turbine was 3927 cm^2, 706.86 cm^2 respectively. Therefore,

$$\text{Area ratio} = \frac{area\ of\ vertical\ axis\ turbine}{area\ of\ horizontal\ axis\ turbine} = \frac{3927}{706.86} = 5.555$$

This ratio affects the torque, velocity, work and power output of the turbines with the same ratio and the same direction of rotation. These values are less than that predicted before as a result to different types and axes of turbines. The velocity of vertical turbine has a smaller area ratio which gives a

correct prediction that the horizontal axis turbine is more efficient. This is in good agreement with literatures.

Figure 8 presentes the upwind and downwind angular velocity findings for the previous measurement days for both wind turbines. It has the same prediction which give an agreement with previous findings of the similar manar curve for higher and lower values. So, it has the same result shown by **Figure** 9 for velocity values for up and downwind.

Equation (13) is used to find the values of actuated velocity of turbines which explained obviously by **Figure 10** which intimates with agreement manar values. It has 2.2 m/s as higher velocity value.

Figure 11 presentes the values of mass flow rate of air calculated by equation 12 that follow the same curves trend for velocity component shown by **Figure 10**.

The kinetic energy of the moving air that is extracted for power production is shown by **Figure 12** which is calculated by equation 11, in addition to the difference in kinetic energy that is calculated by equation 14 for both fans. That curves has the same trend as previous curves of velocity, air mass flow rate etc. because their values is proportional to each other.

Figure 13 presentes the effeciencies of different wind turbines evaluated by (**Wilson, 1994**) that gives the maximum efficieny is less than 60% for ideal optimum wind turbines. This is as a result to many disadvantages and industrial problems of turbines such as the direction of blades to wind, the effect of earth surface to wind velocity and the power transfer.

The mechanical power accumulated by work turbines is dismantled by **Figure 14**. The values of power extracted previously in this figure by calculation of equations 15 or 16. The maximum amount of power is 4.65 Watt for the fifth point of horizontal axis turbine. But, the peak lower value is the first point 0.851 Watt also for the horizontal turbine. This is another prediction for the horizontal turbine to be efficient and favorable.

VALIDITY

The validity of this study is done by applying (**FLUENT and GAMBIT codes, 2008**)on one of turbines (vertical axis wind turbine). **Figure** 1 is drawn schematically in GAMBLT code with tetrahedral cube (150*100*150)cm used as tunnel in which the turbine play. Tetrahedral meshing scheme with 2 interval size is applied to produce 285950 nodes with smoothing and swapping orders. Pressure based, implicit, three dimensions, unsteady, first order, green-gauss node based gradient option and moving mesh with Y-axis rotation direction. Inlet velocity of 2.67m/s in negative Z direction (as shown in **Figure 15**) is selected in this iteration because it is the maximum velocity value resulted by rig readings. The angular velocity is 0.85 rad/s (51rpm). Three levels of surface planes are chosen in horizontal planes to predict the parameters. The lower one at the end edge of turbine when y=0 (Y=y/h=0) as dimensionless scale, the middle plane at y=0.25m (Y=0.5) and the upper (the end) was y=0.5m (Y=1).

Figure 15 shows the turbulent kinetic energy of domain affect the blade with different horizontal position heights. The maximum values take place at the mid plane because it lies inside the effect of blade movement with clockwise rotational direction in impulse direction. The kinetic energy is 2.3 to 3.6 m^2/s^2 in this figure but is 2.355 m^2/s^2 (per unit mass) calculated by practical measurement. This gives good prediction that the validity of study is perfect since the programme code work with ideal condition differ than the practical conditions.

The air pressure impacts the turbine blade area which results a force exerted as shown in **Figure 16** on the open direction to rotate the blade in clockwise direction. This due to the pressure is low on the other side of vane accumulated the first side which shown in **Figure 17** for the same previous slides of horizontal planes. The maximum pressure is 9.62 N/m^2 in B of **Figure 17** and minimum vacuum pressure reachs $19N/m^2$ in rear side of blade in all shapes.

This pressure force leads to move blade in velocity dismanteled by **Figure 18** which gives the same prediction of **Figure 17**. The maximum velocity at the left side of blade to rotate it in clockwise direction (5.23m/s) as shown in B but the minimum near the blade because of the impact and vacuum due to the rotation. The dominated velocity is (2.61- 3.4)m/s which gives good agreement with 2.67m/s (the rig velocity resulted by experimental measurements).
The velocities in X and Y direction shown in **Figure 19** and **Figure 20** that don't give good prediction of movement since they are perpendicular the air movement direction distinguished by reverse Z direction which shown in **Figure 21** where the maximum value is at B on the ends of blade.
The blade velocity for its two sides in Z direction drawn by FLUENT code shown in **Figure 22** to predict the similarity in shape and velocity value for upper part with lower and front with rear. This values were similar to there in **Figure 21**. These give good validity of this study.

CONCLUSIONS:

This practical case study utilized to conclude the following:

1- The earth surface affects the results of wind speed and the rotational movement of turbines to be fluctuated readings. Therefore, the erection of wind mills requires high blades from the earth level.
2- The horizontal axis turbine is efficient than the vertical one (more than 5 depending the area ratio and movement power).
3- The rig models is small scale, therefore the power is very small.
4- The selection of erection position for wind turbine is very important in increasing the power depend the historical measurements of this position.

REFERENCES:

DeCoste J., Smith A., White D., Berkvens D. and Crawford J., (2007) "Self-Starting Darrieus Wind Turbine", Design Project for Mechanical Engineering Department in Dalhousie University.

FLUENT 6.3.26 and GAMBIT code help, (2008).

Hanson, A.C. and Buterfield , C.P., (1993) "Aerodynamics of horizontal –axes wind turbines", Journal of Fluid Mech., 25,115-149.

Johnson G. L., (2006) "Wind Energy Systems", Jon and Willy, USA.

Lian D., Lee J.H. and Kim Y.C., (2010) "Power Prediction Of Darrieus Type Wind Turbine Considering Real Air Velocity On The Wind Turbine Blade", J. of Renewable Energy.

Masse, B., (1986) "A local- circulation model for Darrieus vertical –axis wind turbines", J. Propulsion power 2, 135-141.

Nasuk F.L. and Azumy A., (1983) "An Experimental Verification of the Local Circulation Method for a Horizontal Axis Wind Turbine", paper presented at 18th Intersociety Energy Conversion Engineering Conference, Orlando.

Percival M.C., Leung P.S. and Datta P.K., (2009) "The Development of a Vertical Turbine for Domestic Electricity Generation", Journal of wind engineering.

Schultz C.D., (2009) "The Effect of Gearbox Architecture on Wind Turbine Enclosure Size", AGMA (American Gear Manufacturers Association) Technical Paper, Virginia USA, ISBN: 978--1--55589--97--1.

Sheldahl R.E., (1981) "Comparison of Field and Wind Tunnel Darrieus Wind Turbine Data", Sandia National Laboratories Energy report, USA.

Smith G.A., (1989) "Electrical control methods for wind turbines", winds Eng., 13(2), 88-98.

Stiesdal H., (1999) "The Wind Turbine Components and Operation", an acrobat version of the special issue of the Bonus-Info company, Web: www.bonus.dk.

Wilson R.E. and Spera D., (1994) "Aerodynamic Behavior of Wind Turbines in Wind Turbine Technology, Foundation Concept of Wind Turbine Engineering", ASME press, New York, 215- 282.

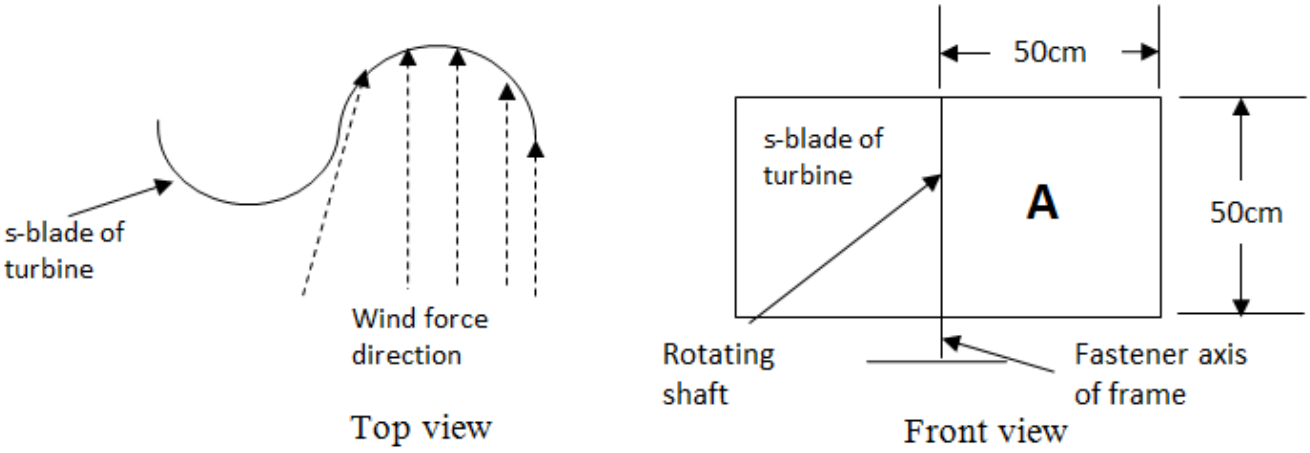

Figure 1 Fabricated rig of Savonius rotor (Vertical Axis Wind Turbine)

Figure 2 Pictures of Savonius rotor (Vertical Axis Wind Turbine) A. Front View, B. Side view, C. Top view, D. Rear view

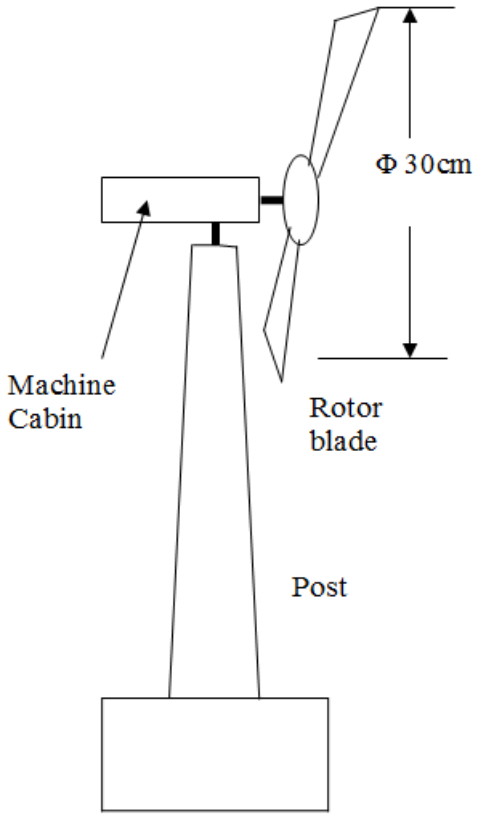

Figure 3 Fabricated rig of Horizontal Axis Wind Turbine.

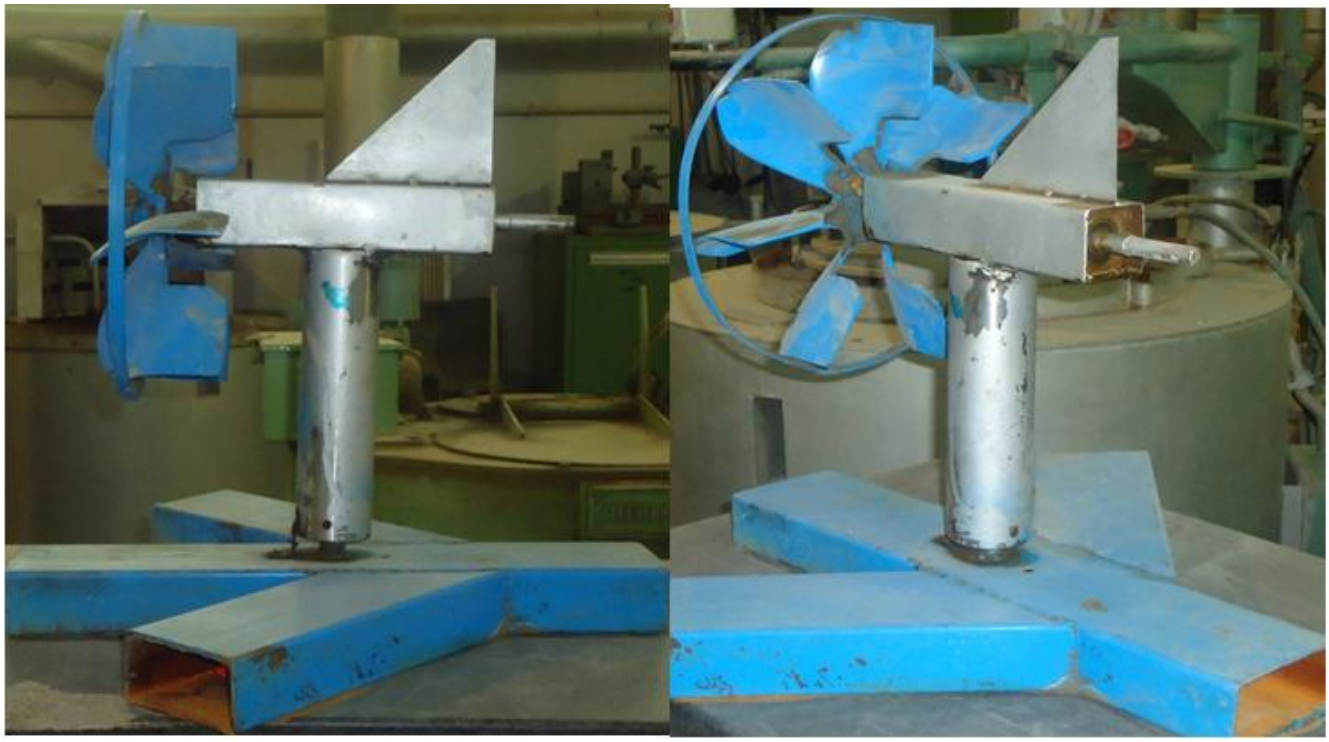

Figure 4 Pictures of Horizontal Axis Wind Turbine

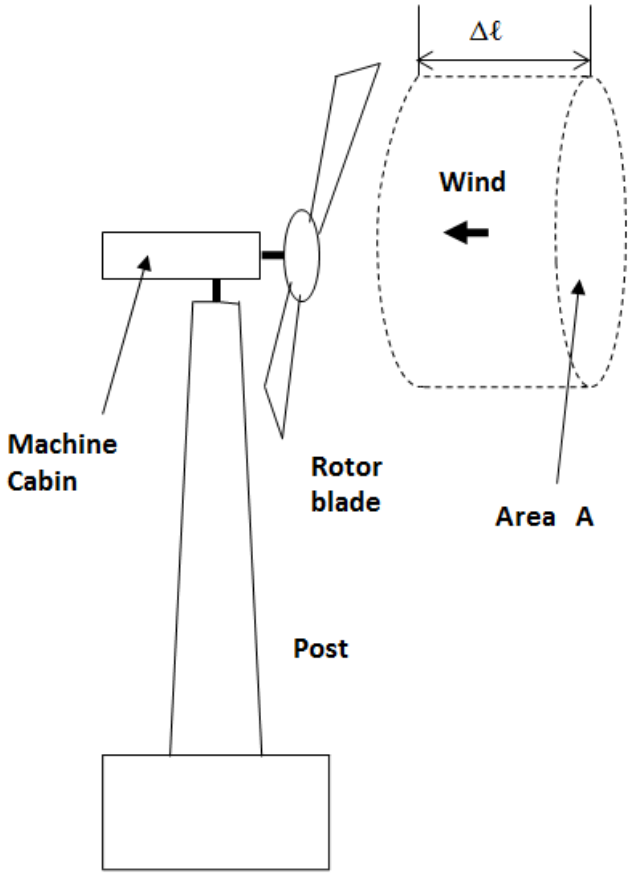

Figure 5 Schematic of horizontal wind turbine.

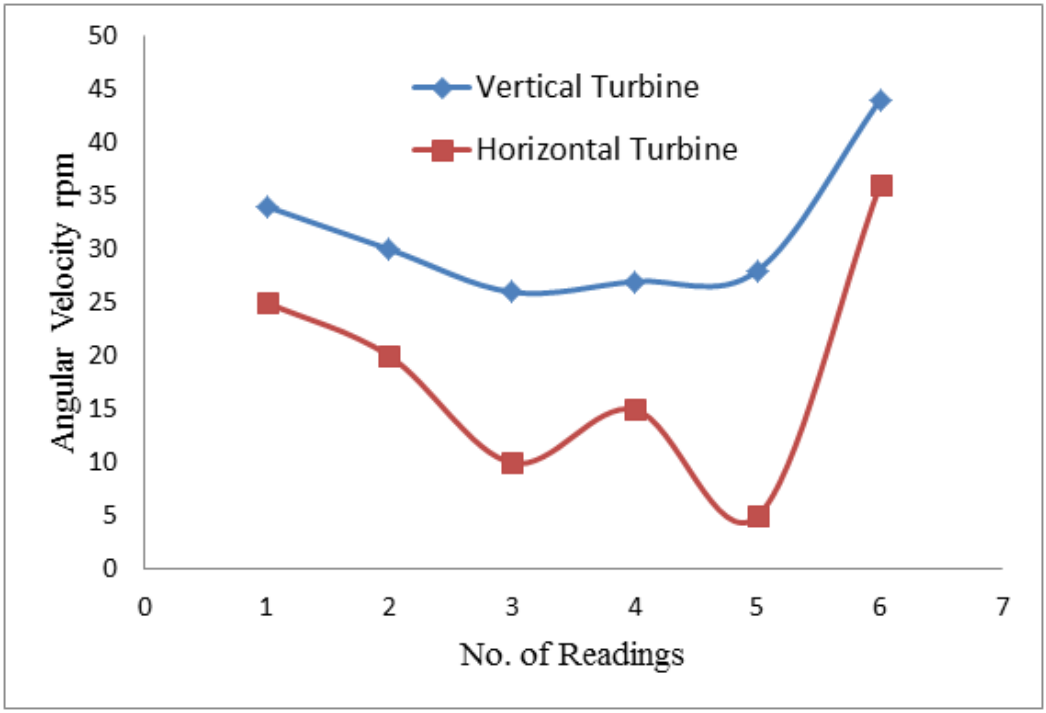

Figure 6 Angular velocity readings for the two turbines on 8th March, 2011

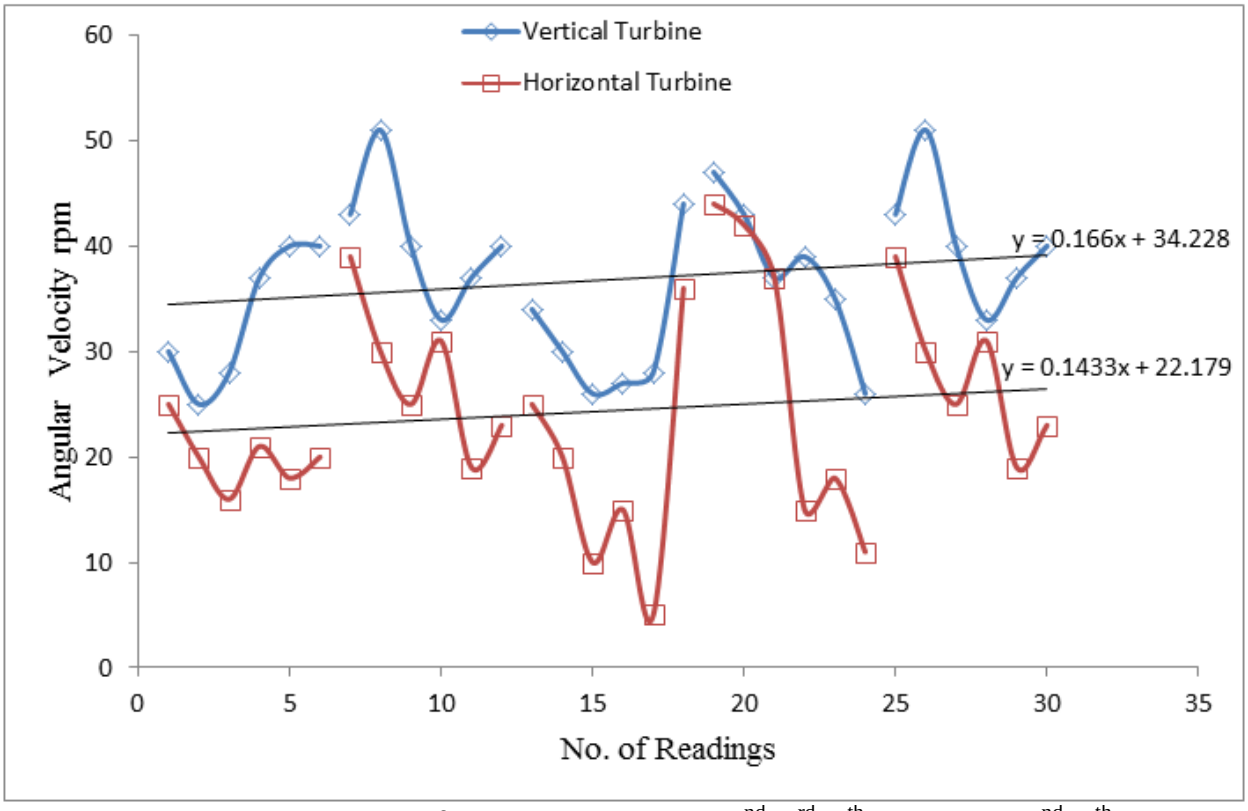

Figure 7 Angular velocity readings for the two turbines in 2nd, 3rd, 8th March and 2nd, 4th April , 2011

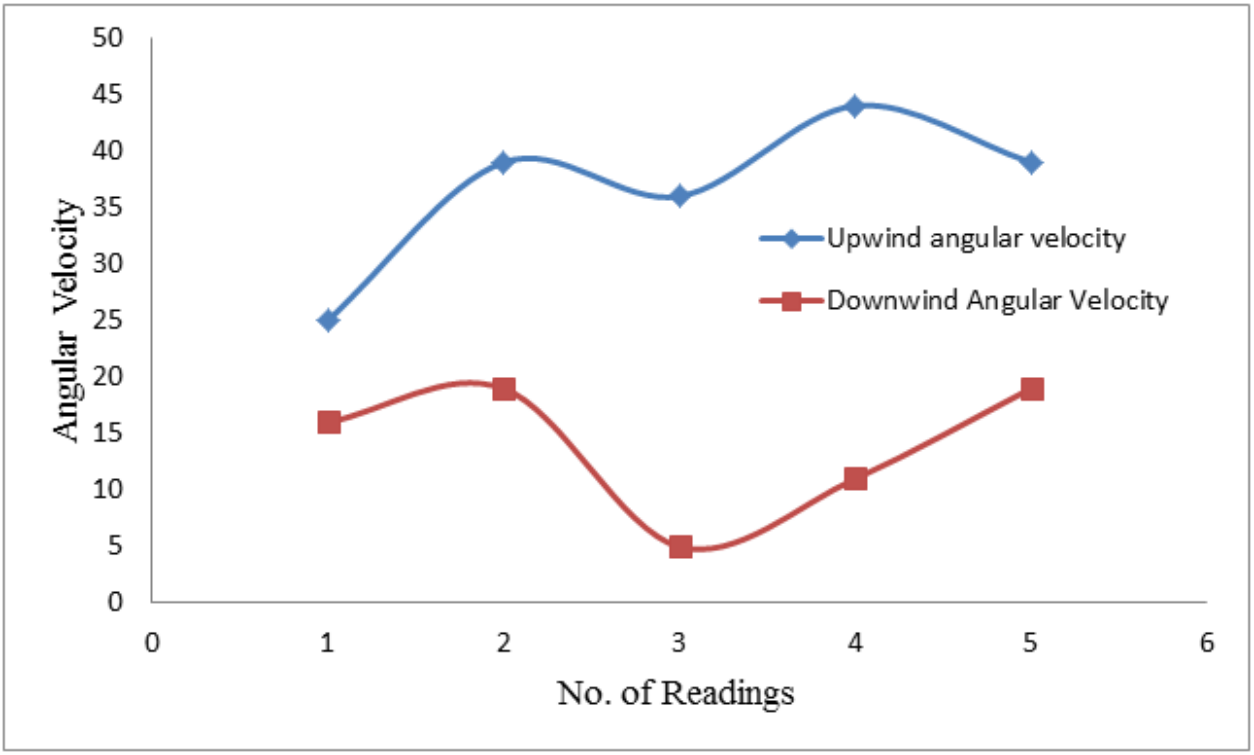

Figure 8 Upwind and downwind angular velocity readings for the two turbines in 2nd, 3rd, 8th March and 2nd, 4th April , 2011

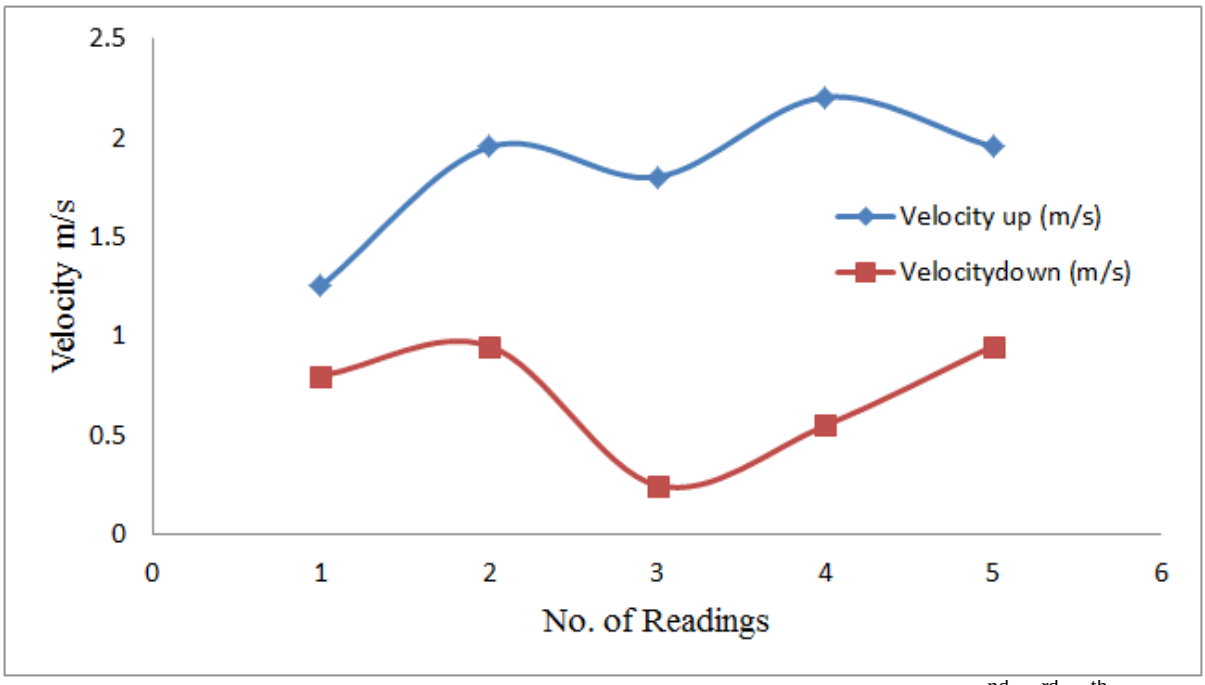

Figure 9 Upwind and downwind velocity (m/s) readings for the two turbines in 2nd, 3rd, 8th March and 2nd, 4th April , 2011

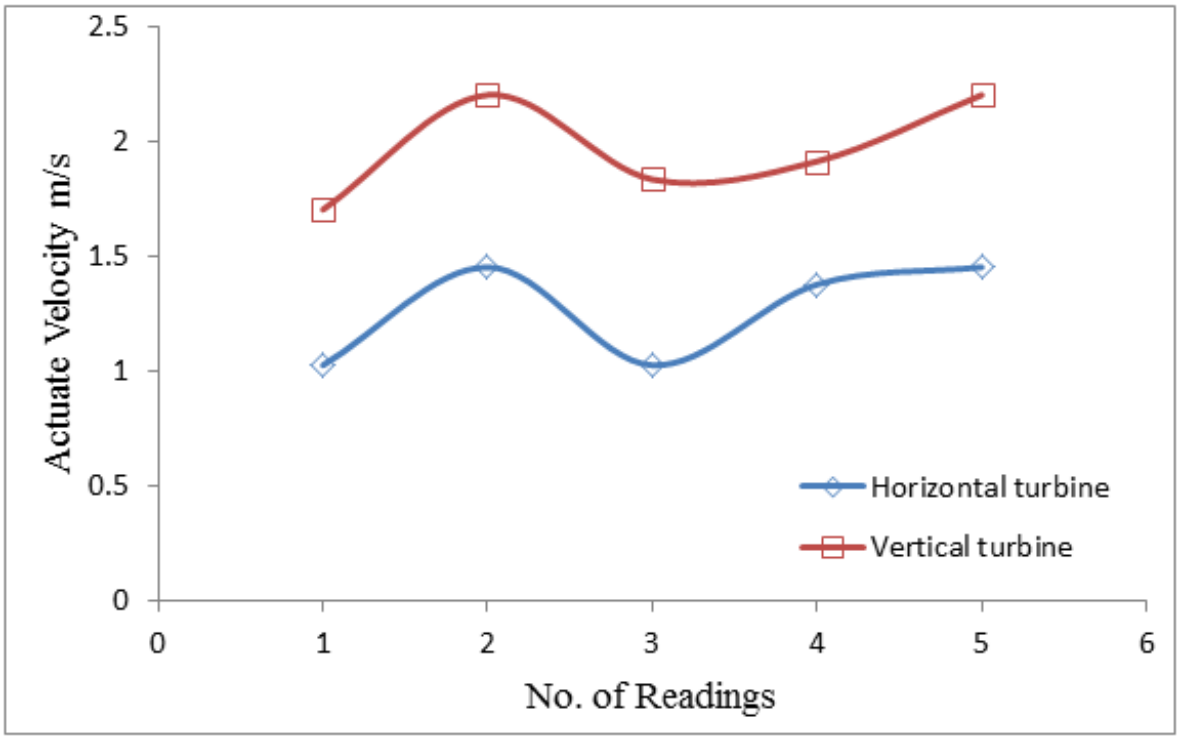

Figure 10 Actuate Velocity (m/s) for the two turbines with different readings days

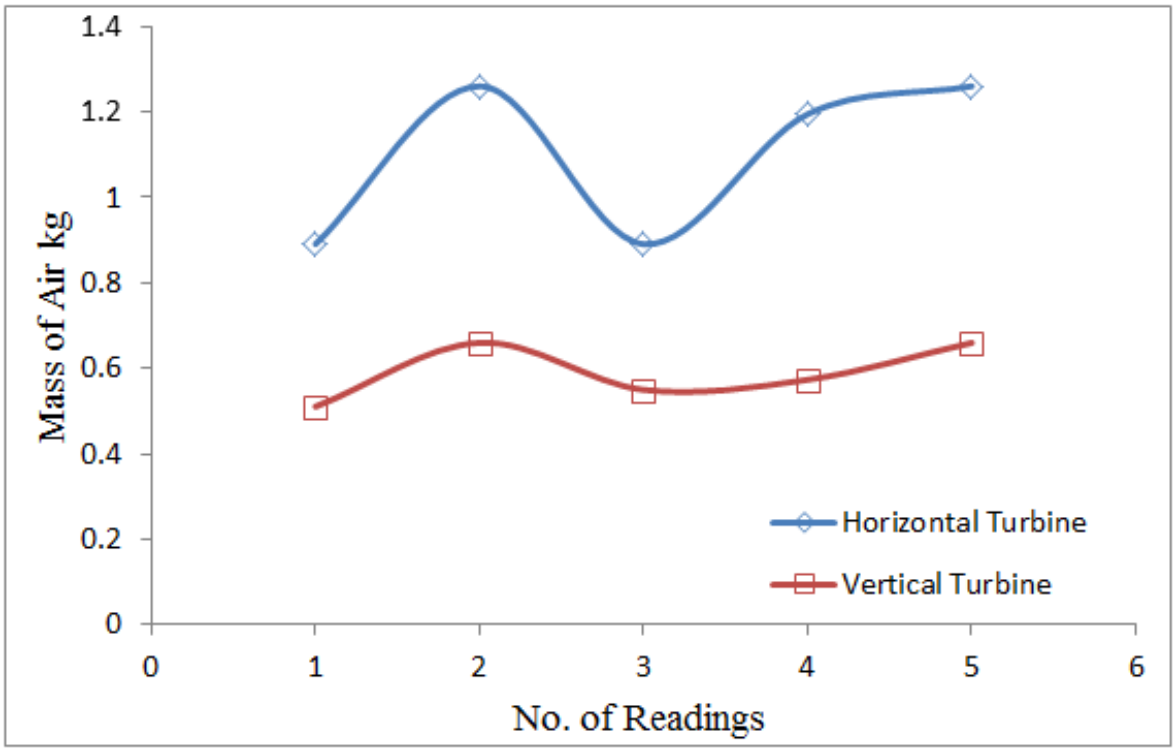

Figure 11 Air mass flow for the two turbines with different readings days

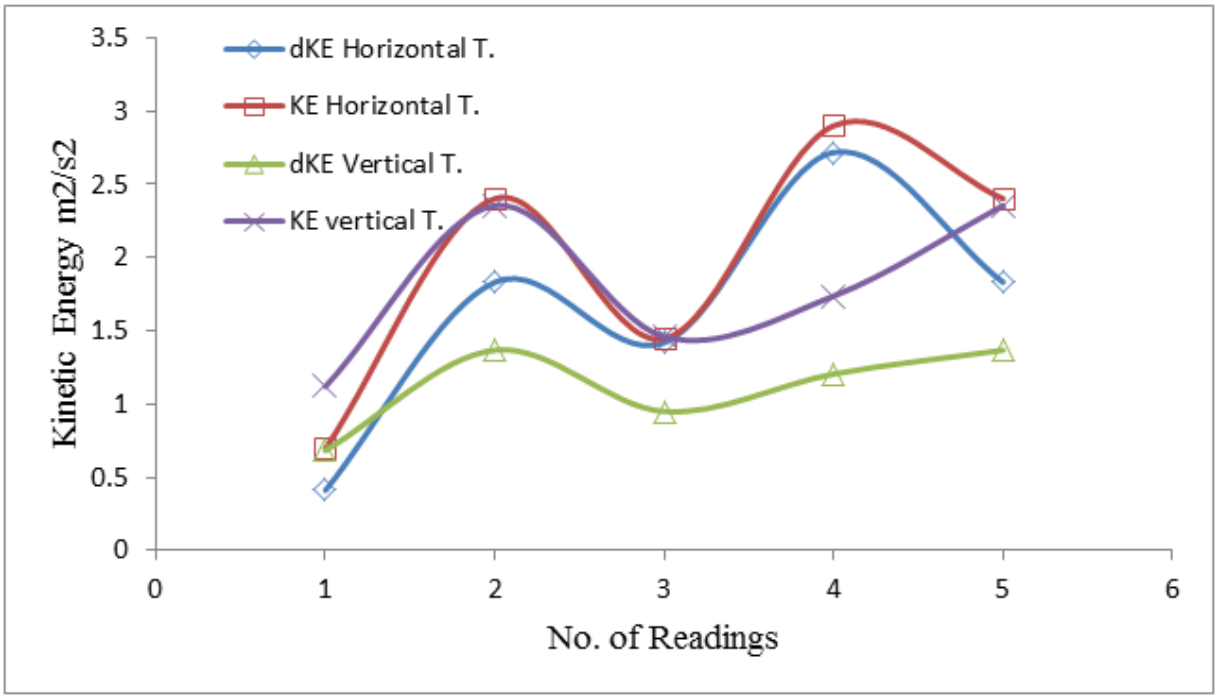

Figure 12 Kinetic Energy (m^2/s^2) for the two turbines with different readings days

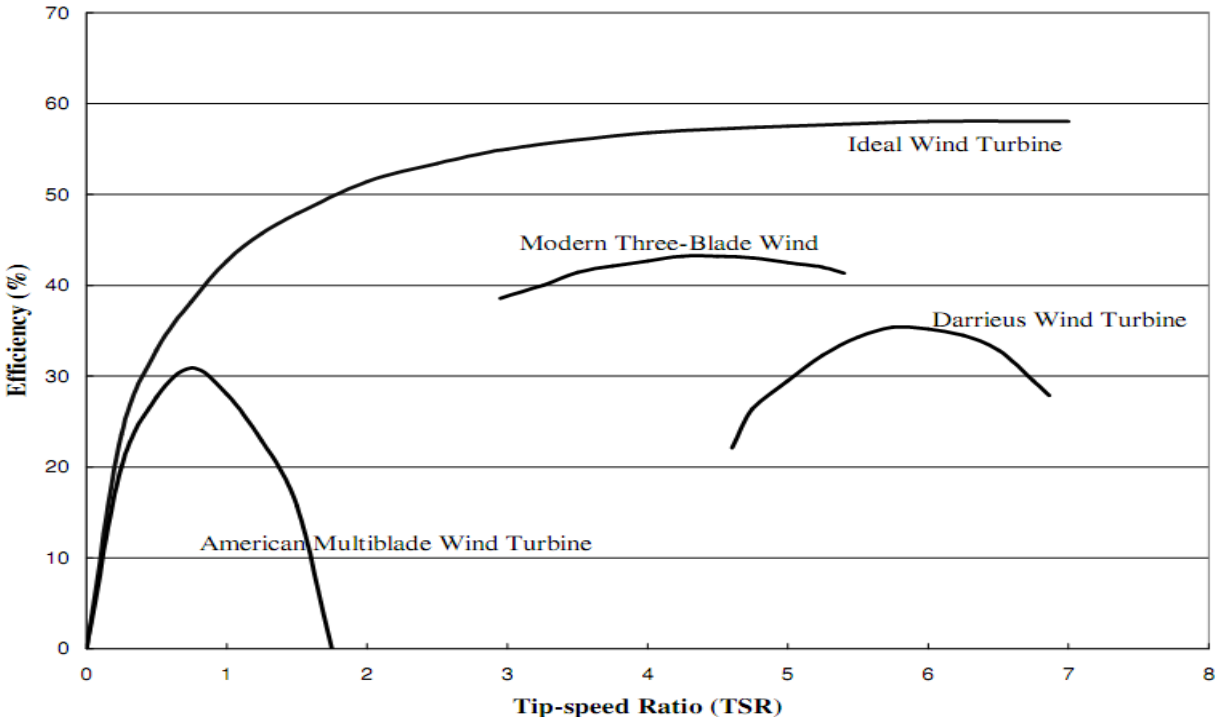

Figure 13 Wind Turbine Efficiencies (Wilson, 1994)

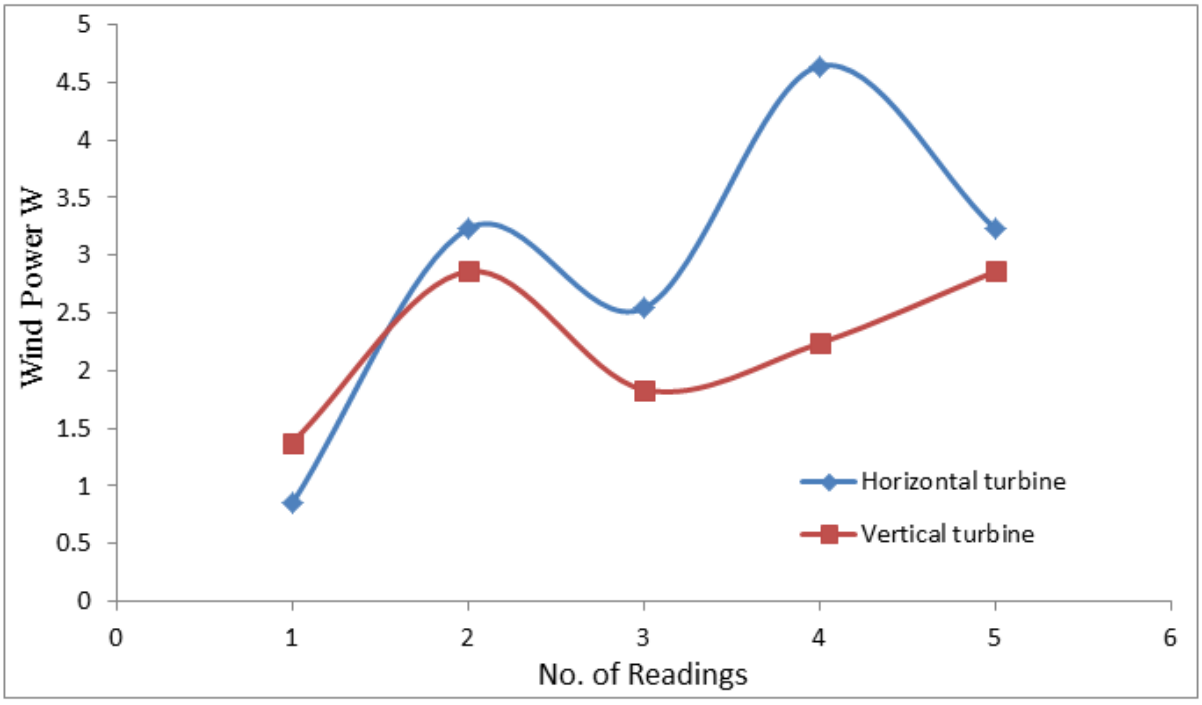

Figure 14 Wind Power for two turbines with different readings days

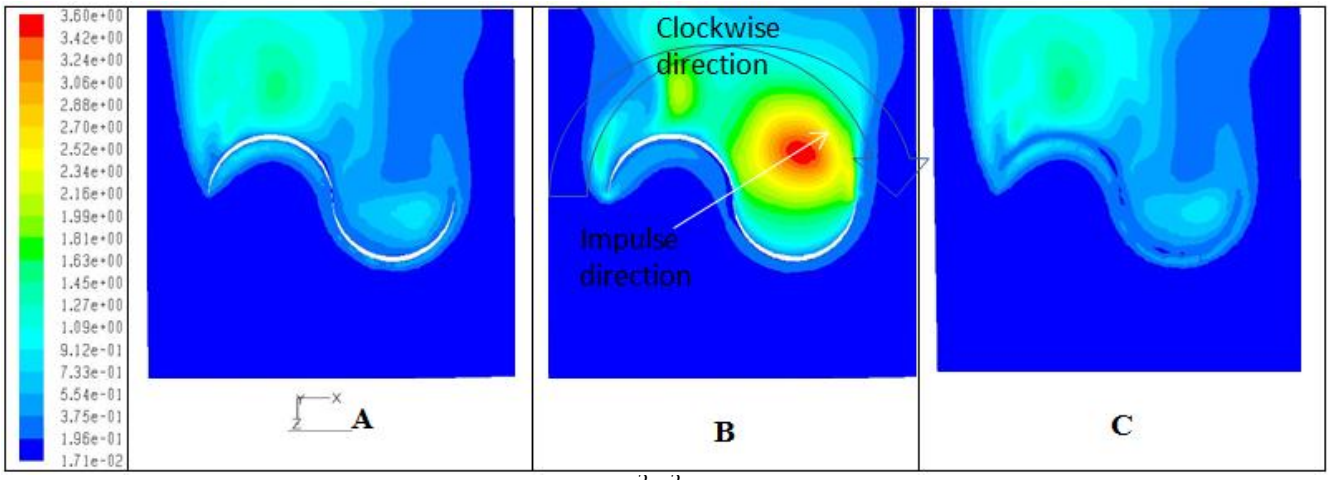

Figure 15 Turbulent Kinetic Energy (m^2/s^2) at A. (y=0), B. (y=0.25m), C. (y=0.5m)

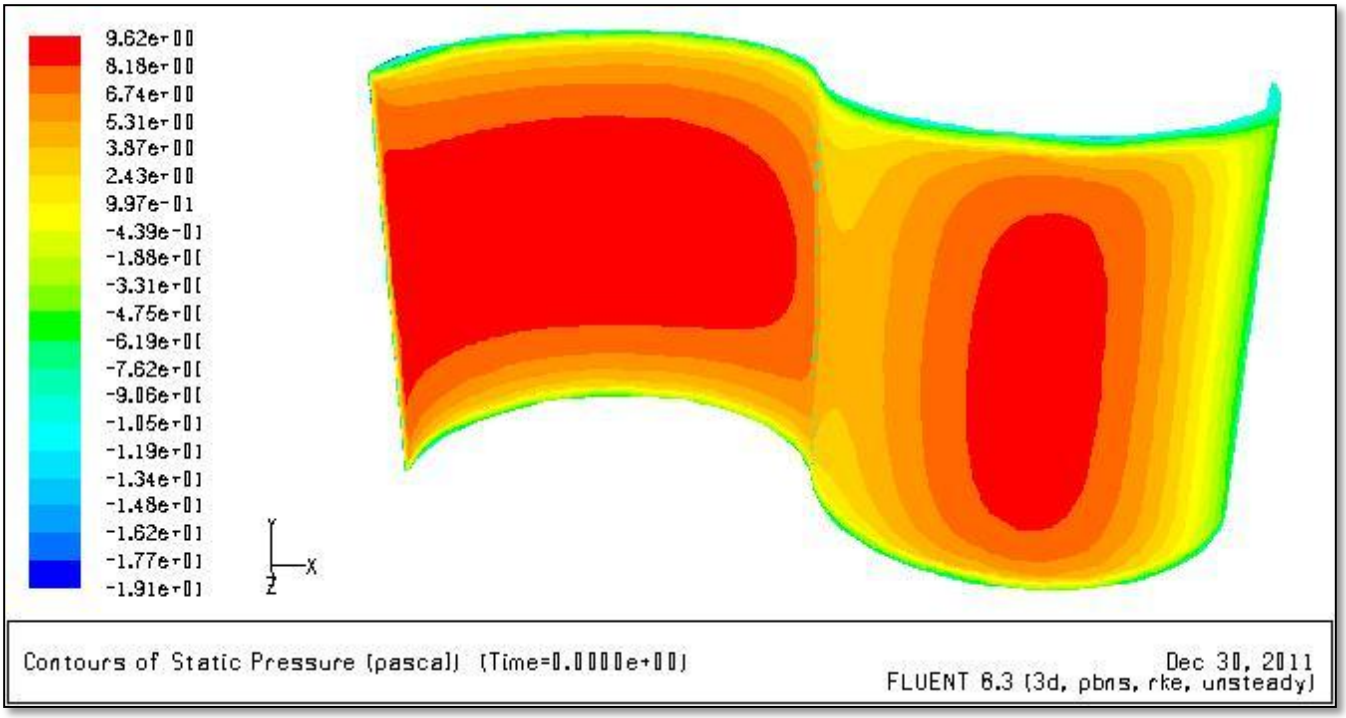

Figure 16 Contour of Static Pressure as shown by FLUENT in Dec 30, 2011

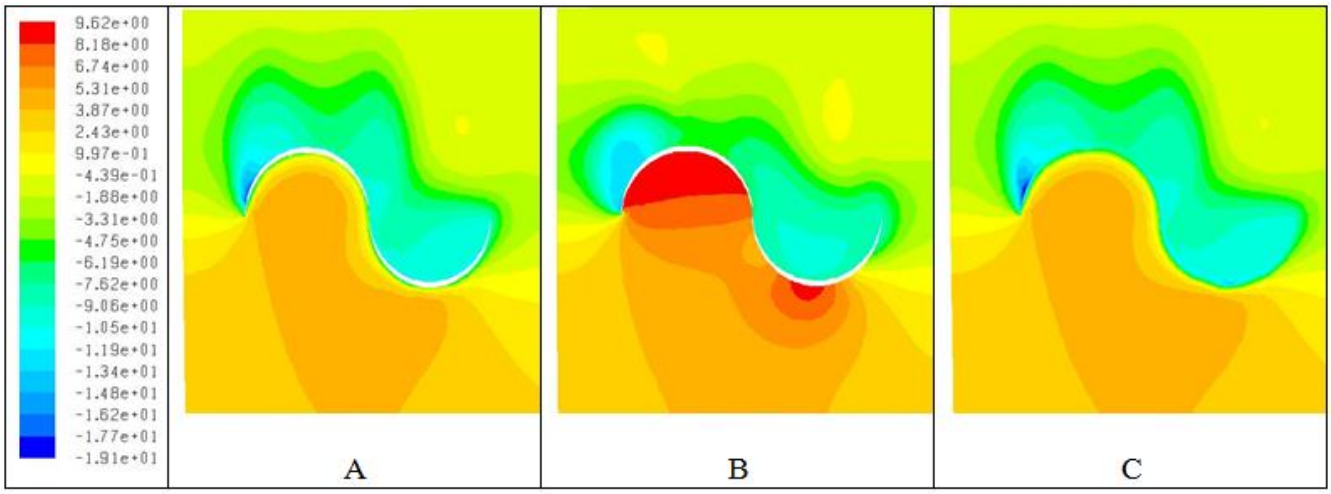

Figure 17 Pressure distribution at A. (y=0), B. (y=0.25m), C. (y=0.5m)

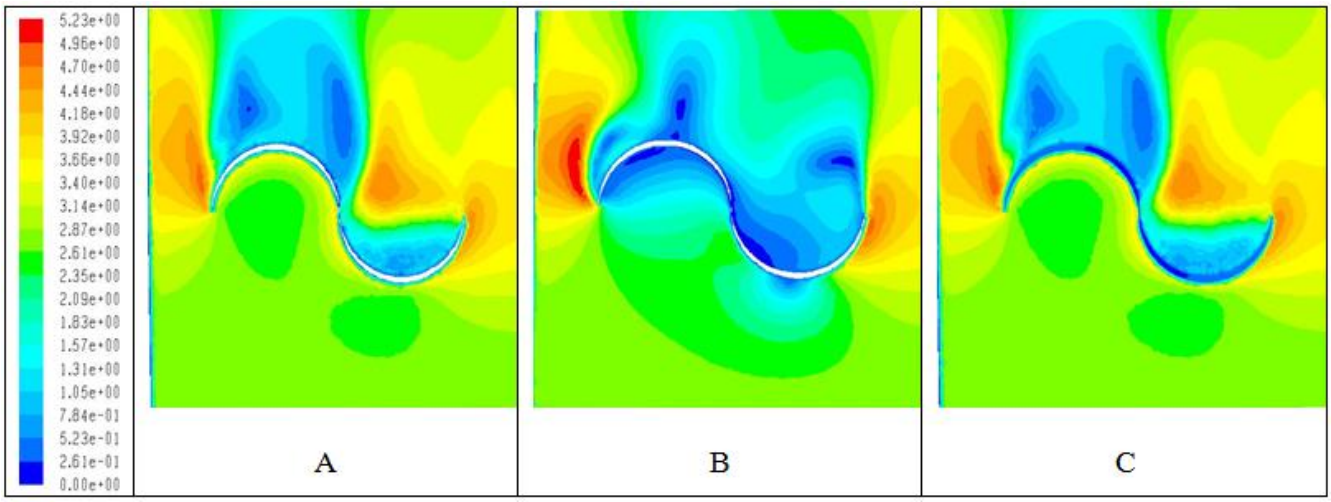

Figure 18 Velocity distribution contour at A. (y=0), B. (y=0.25m), C. (y=0.5m)

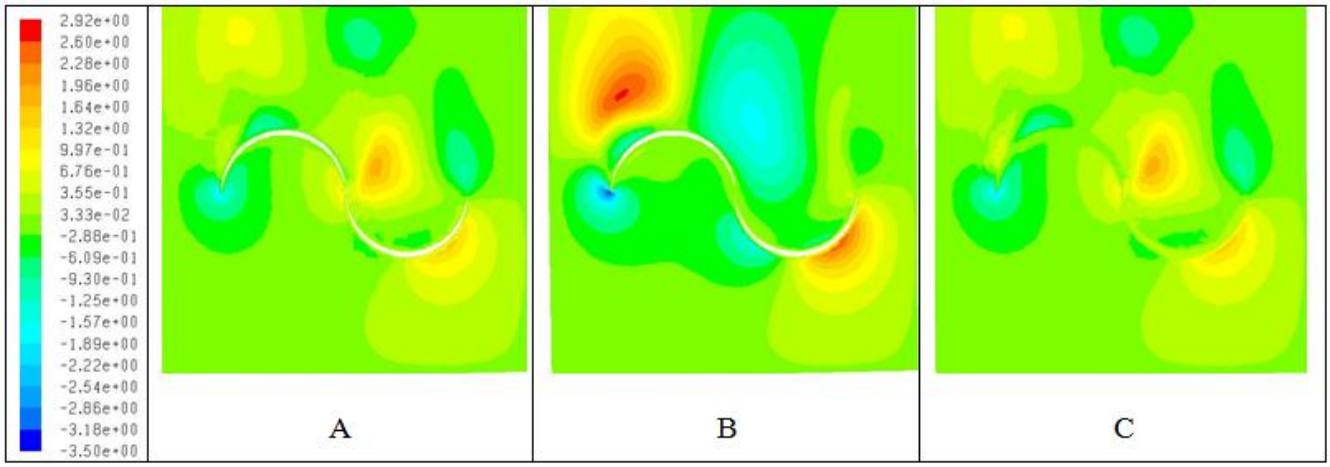

Figure 19 X - Velocity contour at A. (y=0), B. (y=0.25m), C. (y=0.5m)

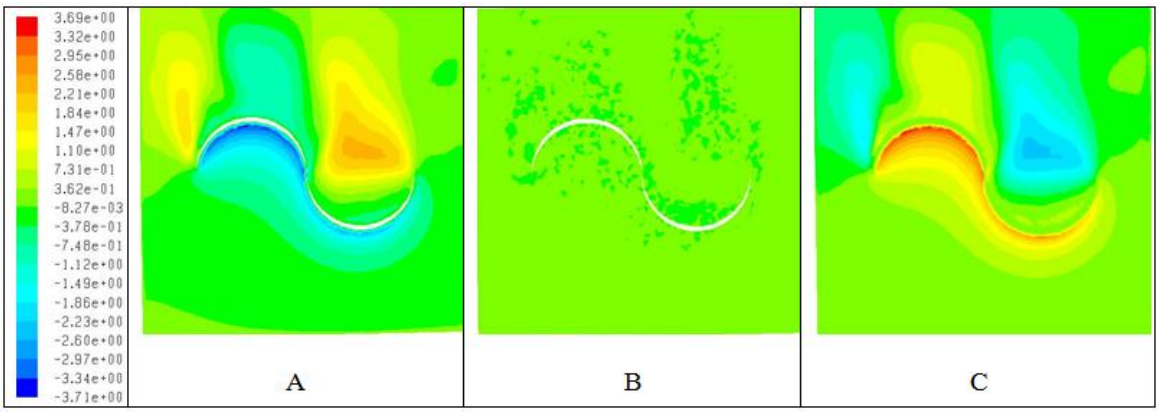

Figure 20 Y - Velocity contour at A. (y=0), B. (y=0.25m), C. (y=0.5m)

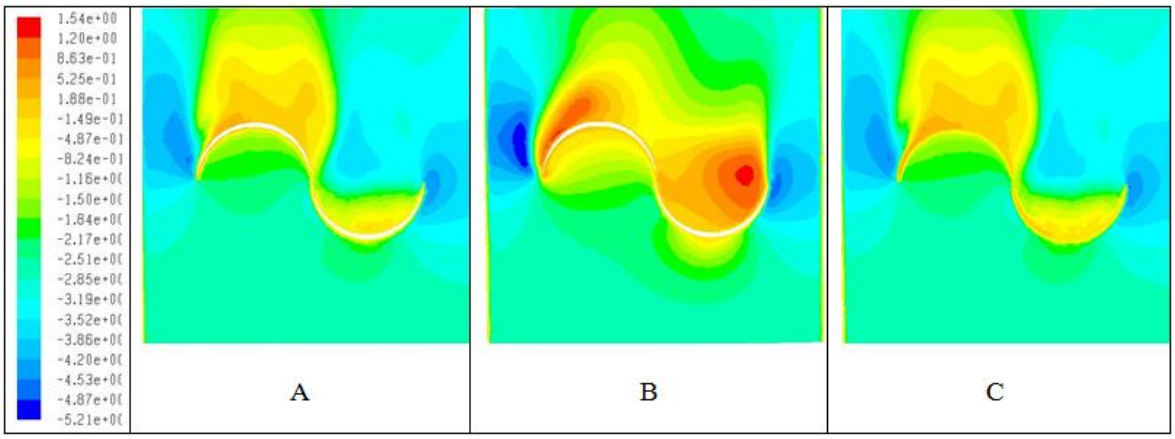

Figure 21 Z - Velocity contour at A. (y=0), B. (y=0.25m), C. (y=0.5m)

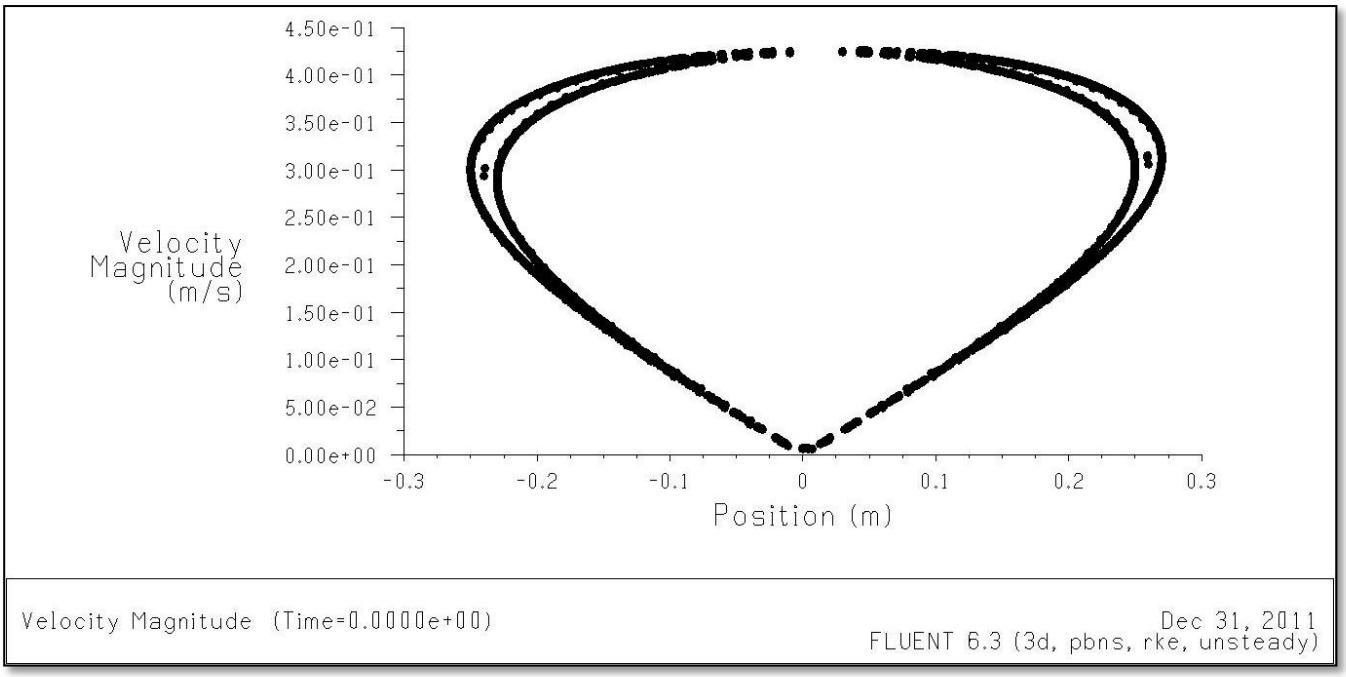

Figure 22 Velocity magnitude curve drawn in Dec. 31, 2011 as shown by FLUENT